Journal of the Physical Society of Japan **86**, 034712 (2017)
https://doi.org/10.7566/JPSJ.86.034712

Combined Effect of External Periodic and Constant Electric Fields on Electron Transport in Carbon Nanotubes and Nanoribbons with Metallic Conductivity

Nail R. Sadykov[1]*, Dmitry A. Peshkov[1], and Pavel N. D'yachkov[2]

[1]*Department of Physics, National Research Nuclear University MEPhI, 115409 Moscow, Russia*
[2]*Kurnakov Institute of General and Inorganic Chemistry of the Russian Academy of Sciences, 119991 Moscow, Russia*

(Received March 11, 2016; accepted January 11, 2017; published online February 27, 2017)

We review the simultaneous effect of AC and DC fields on metallic and semiconductor nanoribbons and nanoribbons with hexagonal structure nanoribbons. Moreover, we define the density of the nonlinear surface current. We find that the amplitude of oscillation in zigzag nanoribbons is exponentially dependent on width and does not depend on width in armchair nanoribbons. The absolute negative conductivity in the nanoribbons was revealed. We define the magnitude of the nonlinear current in the conduction band, taking into account the approaches of dispersion law, based on the first-principle approach.

1. Introduction

Graphene structures are two-dimensional crystalline structures. The presence of an external electric field in the superlattices[1)] leads to different physical effects such as Bloch oscillations, self-induced transparency, negative differential conductivity and absolute negative conductivity.[2,3)] In the case of graphene nanostructures, the period of potential of the crystalline lattice is less than period in the superlattices. Thus, only with large external fields, above mentioned effects will take place in graphene nanostructures.[4–6)]

Under the combined influence of rapidly oscillating AC and DC fields in CNTs, new effects are manifested.[4–8)] The semiclassical theory of the electron transport in the CNTs under the effects of the AC and DC fields is demonstrated.[4,5)]

CNTs are approximately modeled as structures, in which the carbon atoms are arranged along helix, wrapped around cylinder surface.[4)]

Taking into account the real structures of the CNTs and the developed theory,[4)] the propagation of surface waves was reviewed and the nonlinear current was calculated within the kinetic Boltzmann equation by the relaxation time approximation. On the basis of computational and theoretical results, the volt–ampere characteristic of long CNTs in a significant axial DC symmetrical field is presented.[6)]

The differential conductivity for metallic CNTs in the domain of the negative differential conductivity significantly exceeds corresponding values for semiconductor nanotubes.[4)] The simultaneous effect of DC and AC fields leads to the dynamical localization of electrons and self-induced transparency in the case of the resonance radiation in 2D structures, by analogy in semiconductor superlattices.[6)] This also leads to the effect of the absolute negative conductivity that provides a potential for designing generative nanodiodes in microwave and infrared ranges. Analogous results[4–6)] were obtained for nonchiral zigzag and armchair CNTs with metallic conductivity.[7,8)] On the basis of the obtained constant current density in the AC and DC fields in the array of noninteracting CNTs the generation mechanism of radiation in the microwave and terahertz range, is presented.[7)] Comparative analysis of the constant component of the current density in the metallic zigzag and armchair CNTs was carried out.[8)] The absolute negative conductivity was in agreement with the results of numerical calculations.[7,8)] On the basis of the first-principles approach,[9)] the presence of a band gap is set and the dependence the band gap on the graphene nanoribbon width is studied.

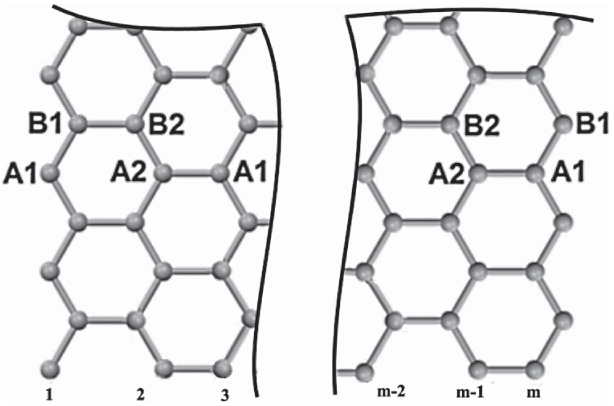

Fig. 1. Network skeleton of the *m*-zigzag nanoribbon.

Bloch oscillations in superlattices with the Stark frequency $\Omega = eE_1 d/\hbar$, where d is the period of the potential in quantum superlattices,[1)] appear under the effect of the DC field ($E_1 = \text{const.}$) in the dispersion law of charge carriers in the form $W \propto \Delta \sin^2(kd/2)$.

In the case of *m*-ZGNR (hereafter denoted as *m*-zigzag nanoribbons, see Fig. 1), the $\xi = ap$ elementary *m*-zigzag cell unit contains $N = 2m$ carbon atoms. Near the Fermi zone, the dispersion law, within the π-electron tight-binding model, has the form $W \sim \Delta \sin^2(kd/2)$, where $m = 1, 2, \ldots$. Such regularity should lead to both quantitative and qualitative changes in the above-mentioned effects. Let us generalize the obtained results for the nanoribbons. The simultaneous effect of AC and DC fields on the metallic and semiconductor nanoribbons, nanoribbons with the hexagonal structure, is reviewed. The densities of the non-linear surface current are defined. The amplitude of oscillation in *m*-zigzag nanoribbons has the exponential dependence on width and does not depend on width in the armchair nanoribbons. The amplitude of oscillation in the metallic nanotubes does not

depend on nanotubes radius. The absolute negative conductivity and self-induced transparency in the nanoribbons are revealed. The magnitude of the nonlinear current was defined taking into account the dispersion law in the conduction band based on the first-principles approaches[9] (see Appendix).

Here, we are interested in large electric field, which lead to the accumulation of the inhomogeneous charge density. Actually, the large values of the electric field, for example, based on the Rashba spin orbit interaction, lead to the appearance of a band gap in metallic nanotubes. This also leads to the interband transitions, what, in turn, should affect the full surface current in nanotubes (see Sect. 5).

2. Constant Component of Current Density

For nanotubes and nanoribbons with the metallic band structure, let us calculate the dependence of the nonlinear current on the magnitude of the electric field[7] in the presence of the alternating and constant-field components. We consider that the largest contribution comes from the conduction band states located near the Fermi level; therefore, we need an explicit form of the dispersion curves in the conduction band crossing the Fermi level E_F and separated from it by an approximate distance $|\varepsilon_c - \varepsilon_F| \leq 0.025$ eV. Within the π-electron tight-binding model, the dispersion curves for nanotubes and nanoribbons are well known. The dispersion curves near ε_F in the case of armchair CNTs (m,m), zigzag CNTs $(m,0)$; armchair nanoribbons m-AGNR (hereafter denoted as m-armchair nanoribbons) have the linear form relating to the translational momentum components $p_z = p$,[10]

$$\varepsilon_{c,v} = \alpha_\pi \pm |\beta_\pi|\chi \sin(\xi - \xi_F); \tag{1}$$

here, $\chi = 1$ for the zigzag CNTs and armchair nanoribbons and $\chi = \sqrt{3}$ for armchair CNTs. It was taken into consideration in Eq. (1) that near the Fermi level ε_F, we have the equality $\sin(\xi - \xi_F) = 2\sin[(\xi - \xi_F)/2]$; "+" and "−" correspond to the valence and conduction bands respectively. Here, for the zigzag CNTs $(m,0)$ with $m = 3q$ and m-armchair nanoribbons, $\xi = ap$, $\xi_F = ap_F = 0$, $a = 3b/(2\hbar)$, $p = \hbar k$, $-\pi/(3b) \leq k \leq \pi/(3b)$, and, for the armchair CNTs (m,m) and m-zigzag nanoribbons, $\xi = \bar{a}p$, $\xi_F = \bar{a}p_F$, $\bar{a} = \sqrt{3}b/(2\hbar)$, $-\pi/(\sqrt{3}b) \leq k \leq \pi/(\sqrt{3}b)$. For the armchair CNTs there is the condition (m,m) $p_F = \hbar k_F = 2\pi\hbar/(3\sqrt{3}b)$ and for the m-zigzag nanoribbons, $p_F = \pi\hbar/(\sqrt{3}b)$. Electron dispersion curves are linear near E_F in the cases of armchair nanotubes and zigzag nanotubes and armchair nanoribbons $\varepsilon_{c,v}(p) = \alpha_\pi \pm \chi|\beta_\pi||\xi - \xi_F|$. It follows from Eq. (1) that the group velocities near the Fermi level for the zigzag CNTs and armchair nanoribbons and for armchair CNTs coincide. The equality of the group velocity near the Fermi level for zigzag CNTs and the armchair CNTs also follows from Fig. 5 in Ref. 10. In this case, it is necessary to consider that, for the zigzag CNTs, the domain of momentum definition is $-\pi/(3b) \leq k \leq \pi/(3b)$, and for the armchair CNTs the domain of momentum definition is $-\pi/(\sqrt{3}b) \leq k \leq \pi/(\sqrt{3}b)$. The equality of the group velocity near the Fermi level for CNTs and for armchair nanoribbons is the same as in Fig. 2 in Ref. 9.

The eigenstates of the m-zigzag $(m \gg 1)$ nanoribbons near ε_F, without considering spins, have a peculiar edge-state structure. As noted earlier, within the tight-binding picture, there are two edge states, decaying into the center of the m-zigzag, with a decay profile depending on their index,[11–14]

$$\varepsilon_{c,v} = \alpha_\pi \pm |\beta_\pi|(2\sin(\xi - \xi_F))^m = \alpha_\pi \pm |\beta_\pi|(2\cos\xi)^m; \tag{2}$$

here, $2\pi/3 < |\xi| < \pi/2$, $\xi_F = \bar{a}p_F = \pi/2$. Equation (2) is received in the case of an arbitrary odd m (see Fig. 1). In agreement with Ref. 15, the group velocity for the conditions with the wave vector $\mathbf{k}$ (defined with respect to the Dirac point) is anisotropically renormalized, i.e., it is a strong function of the direction $\mathbf{k}$. In a 1D superlattice of the Kronig–Penney type of periodic potential with a potential barrier height of 0.5 eV and a spatial period (L) and a barrier width (w) of 10 and 5 nm, respectively, the group velocity of a charge carriers when $\mathbf{k}$ is along a certain direction is renormalized to be less than 40% of its original value. Since the 1D superlattice of the Kronig–Penney type is in fact, a lot of nanotracks, in the case of prolonged m-zigzag nanoribbon, the group velocity along the nanoribbon axis will be also approximately less than 40% of its original value. Despite the anisotropic renormalization of the group velocity for the m-zigzag nanoribbons, here, we use the dispersion law to define the non-linear current, mentioned in Eq. (2), and we use the dispersion law for the real m-zigzag nanoribbons (see Fig. 4 in Ref. 9), which have a narrow gap. Such an approach is justified by the fact, that in both cases the dispersion law for the m-zigzag nanoribbons continues to be applicable.

It follows from the dispersion dependence Eq. (2) that the surface charge density has the following form:[11–14]

$$\Theta_{mg}(\xi) = \Lambda \exp(\alpha(1-m)) \cosh\left[2\alpha\left(g - \frac{m+1}{2}\right)\right],$$
$$\sum_{g=1}^{m} \Theta_{mg} = 1,$$
$$\Lambda^{-1} = \sum_{g=1}^{m} \exp(\alpha(1-m)) \cosh\left[2\alpha\left(g - \frac{m+1}{2}\right)\right],$$
$$\exp(-\alpha) = 2\cos\xi, \tag{3}$$

from the nanotube edge for the g-th zigzag chain (see Fig. 1), where $g = 1, 2, 3, \ldots, m$. In the derivation of Eq. (3), it was taken into account that, if we represent the wave function in the form of a linear combination of atomic orbitals, the surface charge density will be defined by the coefficients at the atomics orbitals $\chi_g^{A_1}$ and $\chi_g^{B_1}$ for odd values of the index g and by the coefficients $\chi_g^{A_2}, \chi_g^{B_2}$ for even values of indexes g in the following forms (see Fig. 1 and Appendix).

$$\sim (|\chi_g^{A_1}|^2 + |\chi_g^{B_1}|^2), \quad \sim (|\chi_g^{A_2}|^2 + |\chi_g^{B_2}|^2).$$

It follows from Eq. (3) that the surface charge density function in the nanoribbons is distributed symmetrically relative to the plane of symmetry. In the point $2\cos\xi = 1$, the surface charge density is a constant in the transversal direction. Equation (3) describes the charge accumulation effect at the ends of nanoparticles. For example, the results shown in Refs. 11–13 are in strong conformity with those shown in Ref. 16. This work shows that Majorana fermions should locate at the ends of a superconducting iron wire. Such quasiparticles are stable and, being sufficiently removed each other, they are not annihilated. In the process of charge

accumulation at the ends of nanoparticles in real devices the observed effects lead to the necessity of considering the ballistic transport of charge carriers:[17–19] the electrical conductance does not depend on the conductor length and it is determined by the conductance quantum $1/R_a$, where $R_a = 12.5\,\mathrm{k\Omega}$. In the charge carrier propagation in nanotubes and nanoribbons when the length of the nanoparticles is $L \le L_0 = 1\,\mu\mathrm{m}$, the ballistic conduction of charge carriers takes place, and when the length of the nanoparticles is $L > 1\,\mu\mathrm{m}$, the movement of charge carriers can be described with the help of the kinetic Boltzmann equation, using the relaxation time approximation $\tau \sim L_0/v_F$. In the case of ballistic conductance, the problem comes down to a charge carrier propagation through the potential barrier, e.g., in carbine chains.[19,20] Accounting of the ballistic conductance allows us to define the transmission coefficient, taking into account boundary conditions at the ends of the nanoparticles. For example, the transmission coefficient depends on the energy of charge carriers relative to the level of energies in carbine chains[19] or nanotubes.[20]

Taking into account the surface charge density Eq. (3), one can define the surface current density using the integral over the first Brillouin zone,

$$j_z = \frac{e}{\pi\hbar}\sum_{g}^{m}\int_{-p_0}^{p_0}\Theta_{mg}(\xi)v_z(\xi)\delta f\,dp, \tag{4}$$

where, the function $\delta f = f(p,z,t) - f_0(p)$ is a small additive to the equilibrium distribution Fermi function f_0, at small values of electric field

$$\delta f = -i\frac{\partial f_0}{\partial p}\frac{eE_z}{\omega + i\nu}. \tag{5}$$

Moreover, the function can be determined using the relaxation time approximation τ from the kinetic Boltzmann equation $f(p,z,t)$,

$$\frac{\partial f}{\partial t} + v\frac{\partial f}{\partial z} + e\tilde{E}_z\frac{\partial f}{\partial p} = -\nu[f - f_0(p)] \tag{6}$$

while taking into account only linear terms relative to the longitudinal electric field E_z and neglecting the field inhomogeneity. In Eq. (6) $\nu = 1/\tau$; $\tilde{E}_z$ is the electric field directed along the Z-axis, consisting of AC and DC fields.

$$\tilde{E}_z = E_1 + E_0\cos\omega t. \tag{7}$$

By taking into account the equality $\sum_{g=1}^{m}\Theta_{mg} = 1$ in Eq. (3), the expression for the surface current in the nanoribbons from Eq. (4) coincides with the expression for the current along the translational Z-axis

$$j_z = \frac{e}{\pi\hbar}\int_{-p_0}^{p_0} v(p)f(p)\,dp. \tag{8}$$

Here, for the zigzag CNTs and m-armchair nanoribbons, $p_0 = \pi/(2a)$; for the armchair CNTs and m-zigzag nanoribbons, $p_0 = \pi/(2\bar{a})$ and $v = \partial\varepsilon_c/\partial p$.

Although the surface conductance of the m-zigzag nanoribbons in accordance with Eq. (4) depends on the y-coordinate (index g),

$$\sigma_{mg} = 8e^2\langle v_{F,g}\rangle/[hH(-i\omega + \nu)],$$
$$\langle v_{F,g}\rangle = \int_{-p_0}^{p_0}\Theta_{mg}(\xi)v_z(\xi)\delta f\,dp, \tag{9}$$

where $h = 2\pi\hbar$ and the index F in $v_{F,g}$ means integration near the Fermi surface. Considering Eqs. (3) and (8), it follows from Eq. (9) that $\sigma_m = \sum_{g=1}^{m}\sigma_{mg}$.

Let us perform the standard transformation $p \to p - eA_z/c$, where c is the speed of light. Assuming that the electrons are distributed uniformly along the Z-axis, we can neglect the second term on the left side of Eq. (6). As a result, in terms of the characteristics method, we obtain[21]

$$f = f_0\left(p + \frac{e}{c}A_z(t)\right)\exp(-\nu t) + \nu\int_{-\infty}^{t}\exp[\nu(t'-t)]f_0\left(\left(p + \frac{e}{c}[A_z(t) - A_z(t')]\right)\right)dt'. \tag{10}$$

Here, $\tilde{E}_z = -\partial A_z/c\partial t$, and A_z is the z-th component of the vector potential. Taking into account Eq. (7), we have $A_z(t) = -cE_1 t - (cE_0/\omega)\sin\omega t$.

Substituting Eq. (10) into Eq. (8) and changing the variables

$$p \to p - \frac{e}{c}[A_z(t) - A_z(t')],$$

one can obtain the expression for current

$$j_z = \frac{e\nu}{\pi\hbar}\int_{-p_0}^{p_0}\int_{-\infty}^{t} v\left\{p - \frac{e}{c}[A_z(t) - A_z(t')]\right\} \times \exp[\nu(t'-t)]\cdot f_0(p)\,dt'\,dp, \tag{11}$$

where, at times greater than the relaxation time, the first term in Eq. (10) is neglected because it is not significant.

Let us consider the Fourier series expansion of the velocity of the charge carriers in Eq. (11),

$$v(\xi) = \sum_l a_l\sin(l\xi), \quad a_l = \frac{1}{\pi}\int_{-\pi}^{\pi} v(\xi)\sin(l\xi)\,d\xi, \tag{12}$$

where ξ is the value determined after Eq. (1). Taking into account the Sommerfeld-integral representation, we have

$$\exp(ix\sin\varphi) = \sum_{n=-\infty}^{\infty} J_n(x)\exp(in\varphi),$$

where $J_n(x)$ is the n-order Bessel function. Equation (11) can be written as

$$j_z = \frac{e\nu}{\pi\hbar}\sum_l a_l B(l,T)\sum_{n=-\infty}^{\infty} J_n\left(\frac{l\nu}{\omega}x_0\right) \times\cos\left(\frac{l\nu}{\omega}x_0\sin\omega t - n\omega t - \varphi_n\right), \tag{13}$$

where

$$B(l,T) = \frac{1}{a}\int_{-\pi/2}^{\pi/2}\cos(l\xi)\left\{1 + \exp\left(\frac{\varepsilon_c - \alpha_\pi}{k_B T}\right)\right\}^{-1}d\xi,$$
$$\sin\varphi_n = 1/\sqrt{1 + (lx_1 + n\omega/\nu)^2}. \tag{14}$$

In Eq. (13) for the zigzag metallic $(m,0)$ nanotubes with $m = 3q+1$ and for the m-armchair nanoribbons with $m = 3q+1$, the values x_0, x_1 have the form

$$x_1 = aeE_1/\nu, \quad x_0 = aeE_0/\nu. \tag{15}$$

Averaging Eq. (13) with respect to time, we obtain an expression for the DC component in the metallic $(m,0)$ zigzag nanotubes with $m = 3q+1$ and in the $(m,0)$ armchair nanoribbons with $m = 3q+1$,

$$j_0 = \frac{e}{2\pi\hbar}\sum_l a_l B(l,T)\sum_{n=-\infty}^{\infty} J_n^2\left(\frac{l\nu}{\omega}x_0\right)\sin 2\varphi_n. \qquad (16)$$

Similar equations for the (m,m) armchair nanotubes and m-zigzag nanoribbons are obtained by substituting a for $\bar{a}$ in Eqs. (15) and (16).

Equation (16) predicts an oscillatory dependence of the constant (time-averaged over the period) component of the current density j_0 on the amplitude of the alternating electric field E_0. This component of the current density through φ_n, in correspondence with Eq. (14), depends on the constant field contribution E_1. The maximum absolute value of the current j_0 achieved at the $\varphi_n = \pi/4$; i.e., under the conditions $\nu = (laeE_1 + n\omega)$ and the minimum value at $laeE_1 + n\omega = 0$. It follows from Eq. (16) that, in the limiting case, when the amplitude of the alternating electric field is equal to zero ($x_0 \to 0$), and a constant electric field influences the system ($E_1 \neq 0$), all the first-kind n-order Bessel functions become to zero, except in the case of $J_0(0) = 1$ and the expression for the nonlinear current Eq. (16) takes the form

$$j_0 = \frac{e}{2\pi\hbar}\sum_l a_l B(l,T)\frac{\nu laeE_1 l}{\nu^2 + (aeE_1 l)^2}, \qquad (17)$$

which coincides with the expression for the current density in CNT in presence of a constant electric field.[6)]

Hereinafter, using the analogy with results of Refs. 3–8 and taking into account Eq. (16), the time-averaged current density oscillations can be written in the form of the function E_0. Such representation of the time-averaged current is convenient, i.e., the conductivity in the nanoribbons oscillates as a function of the amplitude E_0 of the high-frequency field and can be negative. Moreover, a representation of the current density as the function of E_0 with a DC field is convenient in considering some physical problems. For example, the amplitude modulation can be reached using two-frequency carbon dioxide laser radiation (CO_2 laser) or powerful short electrical pulses.[7)]

3. Results of Numerical Calculations

For the zigzag and armchair CNTs, Fig. 2 shows the dependence of j_0 on the amplitude of the alternating electric field E_0. In the calculations, it is assumed that $\omega = 5\nu$, $x_1 = aeE_1/\nu = 4$, and $\nu = 1/\tau$; moreover, the experimental relaxation time[7)] $\tau \approx 3\times10^{-12}$ s is used.

Figure 2 shows that the current density is the oscillating function in the range $\pm10^{-6}$ A. Recall that, according to Eq. (1), the dispersion curve for the (m,m) armchair and $(m,0)$ zigzag CNTs with metallic conductivity near E_F is independent of the m; therefore, j_0 will not depend on the radius in the metallic armchair or zigzag nanotubes.

Now, let us calculate the nonlinear current for m-zigzag ribbons containing $2m$ carbons in a cross section. Then, we have the following expansion of the electron velocity:

$$v(\xi) = \frac{\partial\varepsilon_c}{\partial p} = \sum_l a_l \sin(l\xi). \qquad (18)$$

Equations (2) and (18) show that the coefficients of the Fourier series a_l are different from zero in the case of an even m if the index l is even and $l \le m$; in the case of an odd value m, a_l is nonzero if l is odd and $l \le m$ (see Table I).

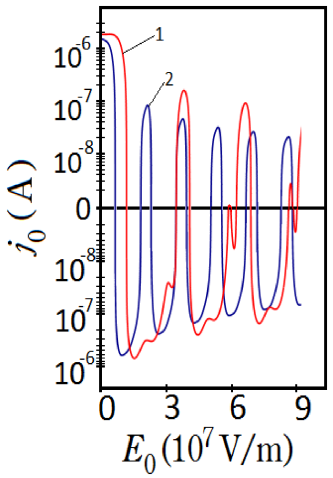

Fig. 2. (Color online) Dependence of the constant component of the current density j_0 Eq. (11) on the E_0 magnitude for the $(m,0)$ and (m,m) CNTs (1 and 2 curves, respectively).

Table I. a_l values for the m-zigzag nanoribbons.

m	$\frac{a_1}{\beta_\pi\bar{a}}$	$\frac{a_2}{\beta_\pi\bar{a}}$	$\frac{a_3}{\beta_\pi\bar{a}}$	$\frac{a_4}{\beta_\pi\bar{a}}$	$\frac{a_5}{\beta_\pi\bar{a}}$	$\frac{a_6}{\beta_\pi\bar{a}}$	$\frac{a_7}{\beta_\pi\bar{a}}$	$\frac{a_8}{\beta_\pi\bar{a}}$	$\frac{a_9}{\beta_\pi\bar{a}}$
2	0	−4	0	0	0	0	0	0	0
3	−6	0	−6	0	0	0	0	0	0
4	0	−16	0	−8	0	0	0	0	0
5	−20	0	−30	0	−10	0	0	0	0
6	0	−60	0	−48	0	−12	0	0	0
7	−70	0	−126	0	−70	0	−14	0	0
8	0	−224	0	−224	0	−96	0	−16	0
9	−252	0	−504	0	−360	0	−126	0	−18

The presence of the coefficients a_l, according to Eqs. (11) and (12) in Table I, allows us to derive an equation that is the generalization of the well-known sine-Gordon equation.[22)]

For the m-zigzag nanoribbons, Fig. 3 illustrates the relationship between the DC component j_0 in Eq. (16) and E_0, calculated for the parameters $\omega = 5\nu = 1.667\times10^{13}$ s^{-1}, $x_1 = 1$. It can be seen from the figure that current density in the range $0 \le E_0 \le 6\times10^7$ V/m also oscillates.

In contrast to the zigzag and armchair nanotubes, the nanoribbons showed an increase m is accompanied by an exponential growth of the amplitude of the current oscillations $j_0(E_0)$. This can be explained by the dependence of the dispersion in Eq. (2).

4. Constant Component of the Current Density Based on the Band Gap for the m-Zigzag Nanoribbons

The nonlinear current for m-zigzag nanoribbons shows a power law dependence on the index m (see Fig. 3). Since, in the case of real m-zigzag nanoribbons, a narrow gap opening appears in the band structure and the qualitative dependence of the structure is retained, it should be expected that for such nanoribbons, the nonlinear dependence of the current on the nanoribbon width remains. The nonlinear current increases according to the power law dependence of the width of the nanoribbons, and thus the impact of the observed narrow energy gap must be compensated. Let us estimate the current density.

To define the nonlinear current in the nanoribbons, one can use the dependence of dispersion[9)] in the conduction band

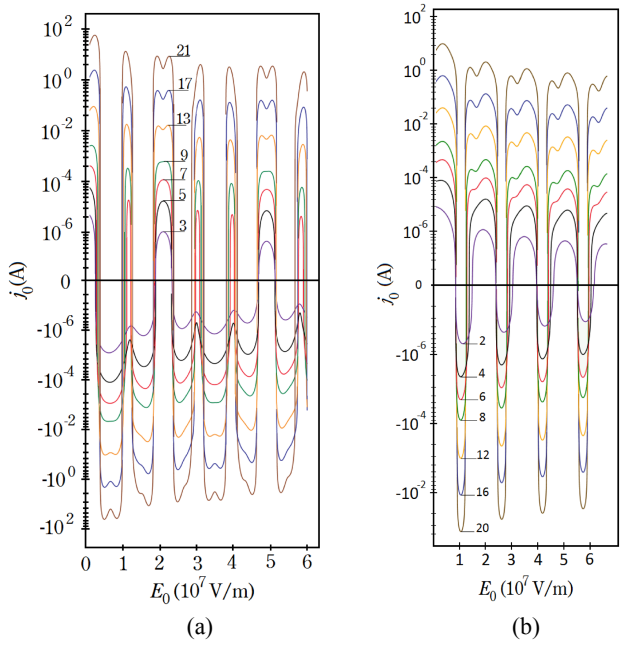

Fig. 3. (Color online) Dependence of the DC component of the current density j_0 on the amplitude of the alternating field E_0 and the odd m (a) and even m (b) values in the m-zigzag nanoribbons.

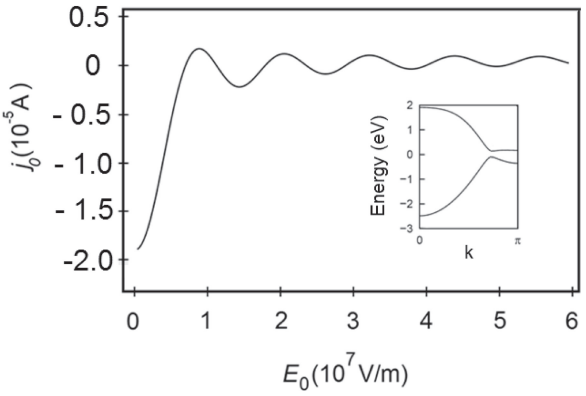

Fig. 4. Dependence of the DC component of the current density j_0 on the amplitude of the AC field E_0 in the 12-zigzag nanoribbons in the presence of the band gap.

(see Fig. 4). Figure 4 shows the dependence of the DC component j_0 in (16) on E_0 at $\omega = 5\nu = 1.667 \cdot 10^{13}\ \mathrm{s}^{-1}$ and $x_1 = 1$ for the m-zigzag nanoribbons at $m = 12$. Figure 4 also shows that, for a changing E_0 in the range $0 \le E_0 \le 6 \times 10^7$ V/m the current density also oscillates. The maximum current is 2×10^{-5} A, which is, according to Fig. 3(b), less than three orders of magnitude than that in the case of 12-zigzag nanoribbons, but greater by one order in contrast to that of the metallic CNTs, according to Fig. 2.

5. Discussion

The modern quantum theory of the quasi-one-dimensional conductors and clusters, being the basis of the description of the electrical properties, predicts the possibility of creating devices (diodes, transistors, and so forth), which will be based on the quantum processes of charge transfer. In the semiclassical approximation for calculating the conductance in quasi-one-dimensional nanostructures, the motion of π-electrons is considered, the dispersion law is taken from the quantum-mechanical model, and the motion of the particle group is described by the classical Boltzmann equation for the distribution function. The applicability of the semiclassical model is limited by the high-frequency domain[23] $\omega \le \bar{\omega} \sim v_F/R_N$ (domain of the optical transitions), where v_F is the speed of π-electrons on the Fermi level and R_N is the nanotube radius. The semiclassical approximation does not consider the interband transitions or quantum-mechanical corrections in the description of intraband motion. By neglecting interband transitions in our problem, we have the condition $\Omega \le \bar{\omega}$, and by neglecting the quantum-mechanical corrections in the description of intraband motion, we have the condition $\hbar\Omega \le \delta E$. Taking into account the evaluation $\delta E \sim |\beta_\pi|$, both limitations for the Stark frequency lead to the limiting DC voltage[6] $|E_1| < |\beta_\pi/2eR_N|$. For the nanoribbons, one can suggest that $2\pi R_N = H$ for to estimate the limiting voltage, and for the m-zigzag nanoribbons, $H = 3bm$. Therefore, at $m = 10$, for the constant electric field, the evaluation $|E_1| \le |\pi\beta_\pi/eH| \sim 10^{10}$ V/m is true. Because in the calculations, it was suggested that $x_1 = aE_1/\nu = 3beE_1/2\hbar\nu = 1$, thus $E_1 = 2\hbar\nu/3bem \approx 3 \times 10^8$ V/m. In this way, the limitations following from this theoretical model, when one neglects the interband transition corrections and quantum-mechanical corrections in the description of the intraband motion, are true. In the frequency domain of the optical transitions the problem of the calculations of the conductivity requires rigorous quantum-mechanical consideration. At the same time, the Coulomb screening effect is significant, which leads to the space nonlocality of the surface conductivity. The quasi-one-dimensional nature of the conductance, unlike volume materials, leads to the features in the manifestation of the Coulomb screening effect.[24–26] In previous papers[27–29] the rigorous quantum-mechanical theory of the conductance in carbon nanotubes, considering the Coulomb screening effect, was developed. In this theory, the Liouville equation must replace the classical Boltzmann equation. The expression for the axial nanotube conductance was obtained in the field linear approximation and in the limiting case of the local response.

In the semiclassical approximation, we do not consider the Coulomb interaction between the electrons. The role of this interaction was reviewed in previous papers.[30–33] It was found that short-range electron–electron interaction is not significantly affected the Coulomb interaction at high temperatures, being typical of the nanotube arrays. Since the Coulomb interaction in separate nanotubes is not screened, it manifests itself in other ways, providing observable effects in a wide range of temperatures. Consequently, the results obtained in our model are predominantly applicable for carbon nanotubes and nanoribbon arrays. For separate prolonged nanoparticles, this model should be changed taking into account the long-range Coulomb interaction. As in Ref. 31, the change in the relaxation dependence $\tau = 1/\nu$, according to the temperature, is the only result of the Coulomb interaction. Because the dispersion curves of the armchair CNT and zigzag nanoribbons practically coincide (two dispersion curves at the edge of the Brillouin zone in the zigzag nanoribbons significantly differ and they coincide with the top of the conductance band in the short-range

approximation), the above is also true for the zigzag nanoribbons.

In Ref. 15, the influence of the external additive periodic field when describing the charge carriers of the two-component wave function was taken into account. Using the results of the first-principles calculations based on the suggested method, the energy dispersion and the group velocities were found, and it was also found that at the border of the minizone the energy-gap openings appear. The group velocity for the expressions with $\mathbf{k}$ (where $\mathbf{k}$ is the wavevector of the Bloch state defined with respect to the Dirac point) is anisotropically renormalized, i.e., it is a strong function of the direction of $\mathbf{k}$; is renormalized to be less than 40% of its original value. We use the method[15] for the narrow prolonged zigzag nanoribbon. In this paper, we are interested in the dispersion curve, in which the conductance band bottom coincides with the conductance band top. Let us suggest that one period of potential energy has the form $U(\mathbf{r}) = -ezE_1$. One can use the first expansion member of the periodic potential energy to the Fourier series

$$U = \sum_G U(\mathbf{G}) \exp(i\mathbf{G}\mathbf{r}) = U(\mathbf{G}_0) \exp(i\mathbf{G}_0\mathbf{r}). \quad (19)$$

From the suggested method in Ref. 15, it follows that in the case of the dispersion curve, from Eq. (19), the energy-gap opening appears,

$$(\varepsilon_{c,v} - \alpha_\pi)^2 = v_F^2\hbar^2k^2 + U^2(\mathbf{G}_0). \quad (20)$$

At $E_1 = 1.6 \times 10^7$ V/m, $L = 10^{-7}$ m, there is $|U(\mathbf{G}_0)| \sim 0.1$ eV. Such an energy gap in the interband transitions corresponds to the infrared radiation frequency, which is significantly greater than the reviewed terahertz radiation frequency $\omega \sim 10^{13}$ s^{-1}.

It should be outlined that a dependence, similar to Eq. (20), can be obtained by taking into account different ways of the Coulomb interaction. Using the convention for Nambuspinors $\Psi = (u_\uparrow, u_\downarrow, v_\downarrow, -v_\uparrow)$, the Hamiltonian in the Bogoliubov–de Gennes (BdG) equations can be reduced to a 2×2 matrix:[34–36]

$$H_0 = H_{\text{kin}} + H_1,$$
$$H_1 = \begin{pmatrix} 0 & V_z + \alpha\partial_x + \lambda\Delta(x) \\ V_z - \alpha\partial_x - \lambda\Delta(x) & 0 \end{pmatrix}, \quad (21)$$

where $v_{\uparrow/\downarrow} = \lambda u_{\uparrow/\downarrow}$, $\lambda = \pm 1$, $H_{\text{kin}} = -(\hbar^2/2m)\partial^2/\partial z^2 - \mu$ is the kinetic energy, the value $V_z = g_{\text{SM}}\mu_B B_z/2$ in-plane magnetic field leads to the spin splitting, $H_{\text{so}} = i\alpha\sigma_y\partial_x$, $\alpha = \mu_0\hbar E_z/mc$, and the phenomenological Rashba parameter α defines the Rashba spin–orbital interaction ($10^{-4} \leq |H_{\text{so}}| \leq 10^{-1}$ eV, see Refs. 39, 37–42), where $\Delta(x)$ is the induced pairing potential in the nanowire. Under the condition $\Delta(x) = 0$ from Eq. (21), we get the dispersion law for 1D Dirac materials that can be described by a single-particle matrix Hamiltonian. In that case, the energy eigenvalues will be equal to $\varepsilon = p_x^2/2m - \mu \pm \sqrt{V_z^2 + (\alpha p_x)^2}$, i.e., the dispersion curve will have an energy gap about 10^{-2} eV. The pairing potential $\propto 10^{-3}$ eV,[43] inducing a superconducting gap, is small, and in our problem, we can neglect this value. Moreover, the considered coherent length ξ (defines the size of the Cooper pairs) is larger than or equal to the nanoribbon length $L \sim 10^{-7}$ m.

Nanowires in the superconducting regime are described by the Hamiltonian BdG, which we will define using the pairing potential. The Hamiltonian BdG describes the Majorana fermions. The stability of the isolated Majorana states to dephasing by the local perturbations is of considerable-applied value, for example, to the electric and magnetic fields and impurities. Such properties make the Majorana fermions attractive in terms of building quantum computers. Taking into account the experimental successes,[44–46] the investigation problem of systems with Majorana fermions becomes actual. On the other hand, the Majorana state inertness and its stability to the perturbations would complicate its experimental detection. Now, the focus is on the transport phenomenon related to the Majorana state. Although the Majorana fermion carries no charge or energy, it, nonetheless, influences the transport properties of the system. Thus, the Majorana state should be visible in the process of the direct measurement of the tunnel state density.[44,47] Note that if the pairing potential is defined by the Coulomb interaction, the Coulomb repulsion leads to a possible magnetic field, based on the Hubbard model within the mean-field approximation.

6. Conclusions

Equation (16) describes the theory of electron transport in the presence of an external electric field $E(t)$ in nanotubes and nanoribbons. We assume that the equations do not take into account interband transitions or quantum-mechanical corrections to the intraband motion or resonant transitions, inherent in the nanotubes and nanoribbon lattices. Figures 2 and 3 show that the amplitude of oscillations of the current density with increasing amplitude of the high frequency also increases, and, in the zeros of the Bessel function (2.4, 4.8, 8.4, 11.8, 14.8, 18.0) the total current is zero (a self-transparency effect). There are fields of the negative differential conductivity and absolute negative conductivity under the influence of the AC and DC fields in nanoribbons and carbon nanotubes. The presence of the absolute negative conductivity must result in the emergence of the absolute negative conductivity zones and active properties of CNTs, providing a potential for the design of generative nanodiodes in microwave and infrared ranges. It was obtained that, in the *m*-zigzag nanoribbons, the amplitude of the oscillations of the non-linear current has an exponential dependence on the width of the nanoribbons. In the armchair nanoribbons, the amplitude of oscillations does not depend on the nanoribbon width and, in the metallic nanotubes, it does not depend on the radius. The the presence of the energy gap in the band structure of the 12-zigzag nanoribbons leads to the increase in the nonlinear current by one order more than that in metallic nanotubes.

Acknowledgment

The authors of the paper would like to thank for the support from National Research Nuclear University MEPhI in the framework of the Russian Academic Excellence Project (contract No. 02.a03.21.0005. 27.08.2013).

Appendix

Let us now define the dispersion law in the vicinity of the Dirac point for *m*-zigzag nanoribbons, where *m* is an odd

number, by analogy with Ref. 13 (see Fig. 1). The system of equations follows from Fig. 1:

$$2\chi_1^{A_1}|\beta_\pi|\cos\frac{kc}{2}\exp\left(i\frac{kc}{2}\right)+\chi_2^{B_2}|\beta_\pi|e^{i\theta}=W\chi_1^{B_1},$$

$$2\chi_2^{B_2}|\beta_\pi|\cos\frac{kc}{2}\exp\left(-i\frac{kc}{2}\right)+\chi_3^{A_1}|\beta_\pi|e^{i\theta}=W\chi_2^{A_2}, \quad (A\cdot1)$$

where $W=\varepsilon-\alpha_\pi$, $c=\sqrt{3}b$, $\theta=\text{const.}$ and the $g=1,2,3,\ldots,m$ indexes of $\chi_g^{A_1}$ and $\chi_g^{B_2}$ values mean the g-th zigzag chain. Near the Fermi point for energy, the $W\to0$ condition is performed.

Let us show that, in the vicinity of the Fermi point for m-zigzag nanoribbons, the dispersion law takes the form

$$W_{c,v}=\pm|\beta_\pi|(2\cos\xi)^m. \quad (A\cdot2)$$

At $W\to0$ from Eq. (A·1), it follows that

$$\chi_m^{A_1}=\left(-2\cos\frac{kc}{2}\right)^{m-1}e^{-i(m-1)\theta}\chi_1^{A_1},$$

$$\chi_1^{B_1}=\left(-2\cos\frac{kc}{2}\right)^{m-1}e^{i(m-1)\theta}\chi_m^{B_1}. \quad (A\cdot3)$$

In the derivation of Eq. (A·3), it was taken into account that the right-hand sides of Eq. (A·1) can be neglected when Eq. (A·2) is performed.

At $W\to0$ from Eq. (A·1), it also follows that

$$2\chi_1^{B_1}|\beta_\pi|\cos\frac{kc}{2}\exp\left(-i\frac{kc}{2}\right)=W\chi_1^{A_1},$$

$$2\chi_m^{A_1}|\beta_\pi|\cos\frac{kc}{2}\exp\left(i\frac{kc}{2}\right)=W\chi_m^{B_1}; \quad (A\cdot4)$$

where in the derivation of Eq. (A·4), in contrast to that of Eq. (A·3), one cannot neglect the the right-hand sides of equalities, since, for the dispersion law Eq. (A·2) all summands in Eq. (A·4) are commensurable quantities. From Eqs. (A·3) and (A·4), it follows that

$$W\chi_1^{A_1}-|\beta_\pi|\left(2\cos\frac{kc}{2}\right)^m\exp(i(m-1)\theta-ikc/2)\chi_m^{B_1}=0,$$

$$-|\beta_\pi|\left(2\cos\frac{kc}{2}\right)^m\exp(-i(m-1)\theta+ikc/2)\chi_1^{A_1}+W\chi_m^{B_1}=0. \quad (A\cdot5)$$

Equation (A·2) follows from Eq. (A·5).

*n.r.sadykov@rambler.ru

1) F. G. Bass and A. A. Bulgakov, *Kinetic and Electrodynamic Phenomena in Classical and Quantum Semiconductor Superlattices* (Nova Science, New York, 1997) p. 498.
2) S. V. Kryuchkov and V. A. Yakovlev, Sov. Phys. Semicond. **10**, 171 (1976).
3) A. A. Ignatov and Yu. A. Romanov, Sov. Phys. Solid State **17**, 3387 (1975); A. A. Ignatov and Yu. A. Romanov, Sov. Phys. Status Solid B **73**, 327 (1976).
4) O. M. Yevtushenko, G. Ya. Slepyan, S. A. Maksimenko, A. Lakhtakia, and D. A. Romanov, Phys. Rev. Lett. **79**, 1102 (1997).
5) G. Ya. Slepyan, S. A. Maksimenko, A. Lakhtakia, O. M. Yevtushenko, and A. V. Gusakov, Phys. Rev. B **57**, 9485 (1998).
6) A. S. Maksimenko and G. Ya. Slepyan, Phys. Rev. Lett. **84**, 362 (2000).
7) N. R. Sadykov, N. A. Scorkin, and E. A. Akhlyustina, Semiconductors **47**, 1246 (2013).
8) S. S. Abukari, S. Y. Mensah, M. Rabiu, K. W. Adu, N. G. Mensah, K. A. Dompreh, A. Twum, and M. Amekpewu, World J. Condens. Matter Phys. **3**, 169 (2013).
9) Y.-W. Son, M. L. Cohen, and S. G. Louie, Phys. Rev. Lett. **97**, 216803 (2006).
10) R. Saito, K. Nakada, M. Fujita, G. Dresselhaus, and M. S. Dresselhaus, Phys. Rev. B **46**, 1804 (1992).
11) M. Fujita, K. Wakabayashi, K. Nakada, and K. Kusakabe, J. Phys. Soc. Jpn. **65**, 1920 (1996).
12) D. J. Klein, Chem. Phys. Lett. **217**, 261 (1994).
13) K. Nakada, M. Fujita, G. Dresselhaus, and M. S. Dresselhaus, Phys. Rev. B **54**, 17954 (1996).
14) N. R. Sadykov, M. B. Belonenko, and D. A. Peshkov, Semiconductors **49**, 663 (2015).
15) C.-H. Park, L. Yang, Y.-W. Son, M. L. Coohen, and S. G. Louie, Nat. Phys. **4**, 213 (2008).
16) A. Y. Kitaev, Sov. Phys. Usp. **44**, 131 (2001).
17) R. Landauer, Philos. Mag. **21**, 863 (1970).
18) M. Büttiker, Phys. Rev. B **46**, 12485 (1992).
19) P. N. D'yachkov, V. A. Zaluev, E. Yu. Kocherga, and N. R. Sadykov, J. Phys. Chem. C **117**, 16306 (2013).
20) N. R. Sadykov, Theor. Math. Phys. **180**, 1073 (2014).
21) E. Zauderer, *Partial Differential Equations Applied Mathematics* (Wiley, New York, 1989) p. 891.
22) Yu. S. Kivshar and B. A. Malomed, Rev. Mod. Phys. **61**, 763 (1989).
23) J. W. Mintmire and C. T. White, Phys. Rev. Lett. **81**, 2506 (1998).
24) M. F. Lin, D. S. Chuu, C. S. Huang, and K. W.-K. Shung, Phys. Rev. B **53**, 15493 (1996).
25) M. F. Lin and D. S. Chuu, Phys. Rev. B **56**, 4996 (1997).
26) M. F. Lin and D. S. Chuu, Phys. Rev. B **57**, 10183 (1998).
27) A. Lakhtakia, G. Ya. Slepyan, S. A. Maksimenko, A. V. Gusakov, and O. M. Yevtushenko, Carbon **36**, 1833 (1998).
28) G. Ya. Slepyan, S. A. Maksimenko, A. Lakhtakia, O. M. Yevtushenko, and A. V. Gusakov, Phys. Rev. B **60**, 17136 (1999).
29) A. S. Maksimenko and G. Ya. Slepyan, in *Electromagnetic Fields in Unconventional Structures and Materials*, ed. O. N. Singh and A. Lakhtakia (Wiley, New York, 2000) p. 217.
30) R. Egger and A. O. Gogolin, Phys. Rev. Lett. **79**, 5082 (1997).
31) C. L. Kane, L. Balents, and M. P. A. Fisher, Phys. Rev. Lett. **79**, 5086 (1997).
32) L. Balents and M. P. A. Fisher, Phys. Rev. B **55**, R11973 (1997).
33) Yu. A. Krotov, D.-H. Lee, and S. G. Louie, Phys. Rev. Lett. **78**, 4245 (1997).
34) R. M. Lutchyn, J. D. Sau, and S. D. Sarma, Phys. Rev. Lett. **105**, 077001 (2010).
35) C. A. Downing and M. E. Portnoi, Phys. Rev. A **90**, 052116 (2014).
36) J. Klinovaja and D. Loss, Phys. Rev. B **86**, 085408 (2012).
37) Y. H. Park, H. Kim, J. Chang, S. H. Han, J. Eom, H.-J. Choi, and H. C. Koo, Appl. Phys. Lett. **103**, 252407 (2013).
38) J. Nitta, T. Akazaki, H. Takayanagi, and T. Enoki, Phys. Rev. Lett. **78**, 1335 (1997).
39) H. Nakamura, T. Koga, and T. Kimura, Phys. Rev. Lett. **108**, 206601 (2012).
40) A. D. Caviglia, M. Gabay, S. Gariglio, N. Reyren, C. Cancellieri, and J.-M. Triscone, Phys. Rev. Lett. **104**, 126803 (2010).
41) S. LaShell, B. McDougall, and E. Jensen, Phys. Rev. Lett. **77**, 3419 (1996).
42) C. Ast, J. Henk, A. Ernst, L. Moreschini, M. Falub, D. Pacilé, P. Bruno, K. Kern, and M. Grioni, Phys. Rev. Lett. **98**, 186807 (2007).
43) A. Chrestin, T. Matsuyama, and U. Merkt, Phys. Rev. B **55**, 8457 (1997).
44) V. Mourik, K. Zuo, S. M. Frolov, S. R. Plissard, E. P. A. M. Bakkers, and L. P. Kouwenhoven, Science **336**, 1003 (2012).
45) A. Das, Y. Ronen, Y. Most, Y. Oreg, M. Heiblum, and H. Shtrikman, Nat. Phys. **8**, 887 (2012).
46) M. T. Deng, C. L. Yu, G. Y. Huang, M. Larsson, P. Caroff, and H. Q. Xu, Nano Lett. **12**, 6414 (2012).
47) K. T. Law, P. A. Lee, and T. K. Ng, Phys. Rev. Lett. **103**, 237001 (2009).